Physical Review A 77, 052312 (2008)

Quantum Entanglement of Formation between Qudits

Seunghwa Ryu[1], Wei Cai[2], and Alfredo Caro[3]

[1]*Department of Physics, Stanford University, California 94305*

[2]*Department of Mechanical Engineering,*

Stanford University, California 94305

[3]*Lawrence Livermore National Lab, Livermore, California 94550*

(Dated: April 15, 2008)

Abstract

We develop a fast algorithm to calculate the entanglement of formation of a mixed state, which is defined as the minimum average entanglement of the pure states that form the mixed state. The algorithm combines conjugate gradient and steepest descent algorithms and outperforms both. Using this new algorithm, we obtain the statistics of the entanglement of formation on ensembles of random density matrices of higher dimensions than possible before. The correlation between the entanglement of formation and other quantities that are easier to compute, such as participation ratio and negativity are presented. Our results suggest a higher percentage of zero-entanglement states among zero-negativity states than previously reported.

PACS numbers: 03.67.Mn, 02.60.Pn

I. INTRODUCTION

Quantum computation and information (QCI) is a new and rapidly growing field at the interface between quantum mechanics and information theory. [1] A major thrust in current QCI research is to build scalable quantum computers that will be able to perform more complex operations and eventually outperform its classical counterparts in certain applications. [2] A quantum computer can outperform a classical computer only through its utilization of quantum entanglement. It has been proved that if the quantum state of a quantum computer has no entanglement, it can do no better than a classical computer.

Entanglement is a fundamental property rooted in quantum mechanics [3] and has been studied extensively in connection with Bell's inequality. [4] A pure state of two quantum sub-systems is called entangled if the wave function of the entire system is unfactorizable, i.e. it cannot be written as a product of the wave functions of the two sub-systems. Consider a quantum system with two sub-systems, A and B, in a pure state that is described by wavefunction $|\psi\rangle$. The entanglement of state $|\psi\rangle$ is defined by the von Neuman entropy of the reduced states,

$$E(|\psi\rangle) = -\mathrm{Tr}\rho_A \log_2 \rho_A = -\mathrm{Tr}\rho_B \log_2 \rho_B, \tag{1}$$

where ρ_A (ρ_B) is the partial trace of the density matrix $\rho = |\psi\rangle\langle\psi|$ over the subsystem B (A). The simplest example for sub-systems A and B are two "qubits", where a qubit is a particle of two linearly independent quantum states (such as the "up" and "down" states of a spin-$\frac{1}{2}$ particle). In this case, the dimension of the Hilbert space of the entire system is $N = 2 \times 2 = 4$; ρ, ρ_A and ρ_B are 4×4, 2×2 and 2×2 matrices, respectively. The sub-systems A and B are called qudits if they are particles with more than two linearly independent quantum states. Hence $N \geq 6$ if at least one of the two subsystems is a qudit.

A mixed state cannot be described by a single wavefunction $|\psi\rangle$ but can still be described by a density matrix ρ. It is always possible to decompose the density matrix ρ into a classical mixture of the density matrices of a set of pure states $|\psi_i\rangle$:

$$\rho = \sum_i p_i |\psi_i\rangle\langle\psi_i|. \tag{2}$$

It is natural to define the entanglement of the mixed state to be the average of the entanglement of pure states $|\psi_i\rangle$, weighted by the probabilities p_i. However, since the decomposition of a mixed state into a sum of pure states is not unique, the above scheme does not give a

unique definition for the entanglement of mixed states. Several entanglement measures of a mixed state have been proposed, among which the entanglement of formation is especially important. [5] It is the minimum entanglement we can get from all possible decompositions,

$$E(\rho) = \min_{\{p_i, \psi_i\}} \sum_i p_i E(|\psi_i\rangle) \tag{3}$$

The entanglement of formation has a simple physical interpretation: it is the minimal amount of entanglement required to create a mixed state with density matrix ρ. [6] In the following, we will refer to the entanglement of formation of a mixed state simply as its entanglement.

Because there are infinite number of ways to decompose a density matrix ρ into a sum of density matrices of pure states, the computation of the entanglement of a mixed state is a non-trivial optimization problem. While the analytic solution has been derived for arbitrary state of two qubits [6] ($N = 4$), no analytical solution is available to date for two qudits ($N \geq 6$). Various algorithms, including Monte Carlo [7], genetic algorithm [8], have been proposed to approach the higher-dimensional problem numerically. Unfortunately, existing numerical methods suffer from slow convergence due to the random nature of their search for the optimal solution, without the aid of local gradient information.

The contributions of this work are twofold. First, a fast, gradient-based algorithm is developed that can be applied to compute the entanglement of qudit systems at higher dimensions than possible before. Second, this new algorithm enables us to gather important information about the "landscape" of the entanglement function and the statistics of the entanglement in the ensemble of random density matrices [7, 9, 10]. Special focus is given to the volume of separable states in the ensemble, i.e. the portion of mixed states which can be decomposed into factorizable pure states (i.e., with zero entanglement). It has been shown that for $N = 4$ and $N = 6$ a density matrix is separable if and only if its partial transpose is positive [11], and these states are called *positive partial transposition* (PPT) states. For $N > 6$, there exist PPT states that have non-zero entanglement, and they are called *bound entangled states*. This suggests that the fraction of separable states among PPT states should be less than 100%. Indeed, for $N = 8$, a previous report estimated the fraction of separable states among PPT states to be 78.7% [7]. Using the more efficient algorithm, we found that the fraction of separable states among PPT states is much larger, actually close to 100% (see Section III C). We believe the difference is due to the better numerical convergence in this work. We also present entanglement statistics for Hilbert

space dimensions up to $N = 16$.

The paper is organized as follows. In Section II, we first set up a standard scheme to decompose an arbitrary density matrix ρ through the use of a unitary matrix $\tilde{U}$, following [6]. Using the expression of derivative of E with respect to U, which is given in Appendix A, we then present three gradient search algorithms: steepest descent, conjugate gradient, and a hybrid method. Some benchmark data illustrating the convergence and efficiency of the three methods and the nature of the "landscape" of the entanglement function are also presented in Section II. Using the hybrid method, Section III presents the entanglement statistics in ensembles of random density matrices at higher dimensions than what is numerically achievable before. A summary and a outlook for future work are presented in the last section. The appendices provide more details on the derivation of the gradient direction, and the method of imposing constraints during the optimization.

II. GRADIENT SEARCH ALGORITHMS

A. Mixed state decomposition using unitary matrix

Consider an $N \times N$ density matrix ρ. Because it is a positive semi-definite Hermitian matrix, it can always be diagonalized by a unitary transformation,

$$\rho = VDV^\dagger \tag{4}$$

where V is a unitary matrix, and D is a diagonal matrix with $D_{ii} = \lambda_i \geq 0$. Define another diagonal matrix C such that $C_{ii} = \sqrt{\lambda_i} \geq 0$, and matrix $\tilde{V} \equiv VC$, then

$$\rho = VCCV^\dagger = \tilde{V}\tilde{V}^\dagger, \tag{5}$$

Now consider an arbitrary unitary matrix $\tilde{U}$ with dimension $M \times M$ where $M \geq N$. We can construct an $M \times N$ matrix U from the first N columns of $\tilde{U}$, where $U^\dagger U = I_{N\times N}$. Using $\tilde{U}$ we can rewrite matrix ρ as,

$$\rho = \tilde{V}U^\dagger U\tilde{V}^\dagger = WW^\dagger = \sum_{i=1}^{M} w_i\, {w_i}^\dagger, \tag{6}$$

where $W \equiv \tilde{V}U^\dagger$ is an $N \times M$ matrix, and w_i are column vectors of matrix W, i.e. $W = [w_1|w_2|\cdots|w_M]$. Each column vector w_i is a vector of dimension N, but is not necessarily

normalized. Define the normalization constant $p_i \equiv {w_i}^\dagger w_i$. Now each normalized vector $\tilde{w}_i = w_i/\sqrt{p_i}$ corresponds to a pure state (i.e. a wave function) in the N-dimensional Hilbert space. The density matrix ρ can now be written as a sum of these pure states. In Dirac's notation, $\tilde{w}_i \equiv |\tilde{w}_i\rangle$ and $\tilde{w}_i^\dagger \equiv \langle\tilde{w}_i|$. Hence

$$\rho = \sum_{i=1}^{M} p_i \, \tilde{w}_i \, \tilde{w}_i^\dagger = \sum_{i=1}^{M} p_i \, |\tilde{w}_i\rangle \, \langle\tilde{w}_i|. \tag{7}$$

It has been shown that an arbitrary decomposition can be described by the above scheme with a suitable choice of unitary matrix $\tilde{U}$. The entanglement given by this decomposition is a function of both ρ and U (the first N columns of $\tilde{U}$). Computing the entanglement of formation of matrix ρ is then an optimization problem,

$$E(\rho) = \min_{U^\dagger U = I} E(\rho, U) \tag{8}$$

where

$$E(\rho, U) = \sum_{i=1}^{M} p_i E(|\tilde{w}_i\rangle), \tag{9}$$

The freedom of choosing the matrix U means that there are infinitely many ways to decompose a mixed state density matrix. The dimension M of the unitary matrix $\tilde{U}$ dictates the number of pure states that ρ will be decomposed into and M can be arbitrarily large. Fortunately, it has been shown that there is no need for M to exceed N^2 [14] (in the sense that it will not give rise to decompositions with different values of entanglement). Furthermore, the decomposition given by all unitary matrices of dimension $M_1 \times M_1$ is a subset of decompositions given by all unitary matrices of dimension $M_2 \times M_2$ if $M_1 < M_2$. Therefore, the search for the optimal matrix U is limited to the dimension of $N \times M$ where $M = N^2$. In practice, we find that the minimized value for E converges quickly as a function of M so that there is no need to go to the upper bound of $M = N^2$.

The information above is sufficient to construct a Monte Carlo algorithm to minimize E with respect to all admissible matrices U. [7] The algorithm consists of a trial step in which various components of matrix U is perturbed randomly and the trial is accepted or rejected based on the resulting change in E. However, this algorithm is very slow because of its random nature of the search for a better candidate matrix U. It is well known that an optimization algorithm becomes much faster if it can take advantage of the local gradient information. For this purpose, we have obtained the explicit expressions for the partial

derivatives of E with respect to every component of matrix U,

$$G_{ij} \equiv \frac{\partial E(\rho, U)}{\partial U_{ij}} \tag{10}$$

The results and derivations are given in Appendix A.

B. Minimization with constraint

The information about the local gradient G_{ij} can be used to construct more efficient search algorithms for the optimal decomposition matrix U. Care must be taken to account for the constraint that U is the first N columns of a unitary matrix. In other words, the columns of matrix U are normalized vectors that are orthogonal to each other. This situation is very similar to quantum *ab initio* calculations [12] for which both steepest descent and conjugate gradient algorithms have been successfully developed to solve the ground state electron wave functions. In the following, we describe the steepest descent and conjugate gradient algorithms to compute the quantum entanglement, which are motivated by this analogy.

Because the dimension of our system is much smaller than that in *ab initio* simulations [12] (a few versus a few thousand), we use a different way to impose the ortho-normal constraints during the optimization. Instead of explicitly normalizing and orthogonalizing the column vectors, we rewrite the unitary matrix as an exponential of a Hermitian matrix,

$$\tilde{U} = e^{iH}, \tag{11}$$

where the constraint $H = H^\dagger$ is much easier to impose. At each iteration, when the new Hermitian matrix in the next step becomes,

$$H^{\rm new} = H + \delta H \tag{12}$$

the resulting new matrix

$$\tilde{U}^{\rm new} = \tilde{U}\, e^{i\delta H} \tag{13}$$

is guaranteed to be a unitary matrix. [18]

C. Steepest descent algorithm

If there were no constraints on matrix U, a steepest descent (SD) algorithm would update U_{ij} at each step along the steepest descent direction $d_{ij} = -G^*_{ij}$, where * represents complex

conjugate. In matrix notation,

$$\tilde{U}^{\rm new} = \tilde{U} + \lambda\, d \tag{14}$$

where λ is a small step size parameter.

To impose the unitary constraint, we employ the transformation in Eqs. (11)-(13) and let

$$\delta H = \lambda\, g \equiv \frac{\lambda}{2}\left[\left(i\tilde{U}^{\dagger}\tilde{G}^{*}\right) + \left(i\tilde{U}^{\dagger}\tilde{G}^{*}\right)^{\dagger}\right] \tag{15}$$

where $\tilde{G}$ is a $M \times M$ matrix whose first N columns comes from N columns of G and other components are filled with zeros. The fact that matrix g is the steepest descent direction for matrix H is shown in Appendix B.

In our steepest descent algorithm, the value of λ is allowed to adjust automatically during the iterations. At each SD step, the value of λ is initialized to be the value from the previous step. Given this step size, if $E(\rho, U^{\rm new}) > E(\rho, U)$, we then divide λ by 2 until $E(\rho, U^{\rm new}) < E(\rho, U)$. If, on the other hand, $E(\rho, U^{\rm new}) < E(\rho, U)$, we then try to double λ and the trial is accepted if this gives rise to an even lower value for $E(\rho, U^{\rm new})$.

Fig 1(a) illustrates the trajectory of a typical SD minimization for a test case of a two-qubit system. The trajectory exhibit a highly zig-zag shape as it approaches the minimum, which significantly slows down the convergence speed of the SD algorithm near narrow landscape of the objective function. [13]. This is a well known problem and is precisely the motivation for the development of a conjugate gradient algorithm in *ab initio* calculations. [12]

D. Conjugate gradient algorithm

The conjugate gradient (CG) algorithm finds the minimum of a function through a series of searches. In each search the algorithm determines the minimum of the function along a search direction. The search direction is computed based on the local steepest descent direction but also has to be "conjugate" to all previous search directions. The CG algorithm works especially well when the local landscape is quadratic. CG generally outperforms SD in complex nonlinear landscapes as well. [13] At the beginning of the n-th iteration, given the local steepest descent direction $g^{(n)}$ (for matrix H defined in Eq. (11)), the new search

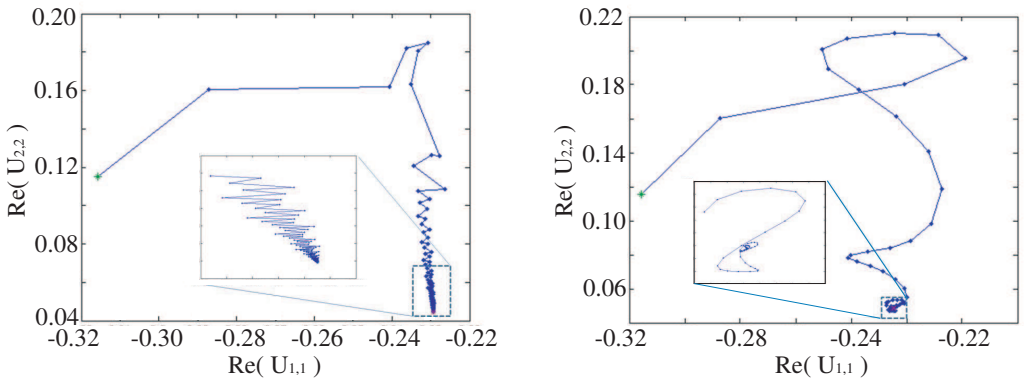

(a)Steepest descent (b)Conjugate gradient

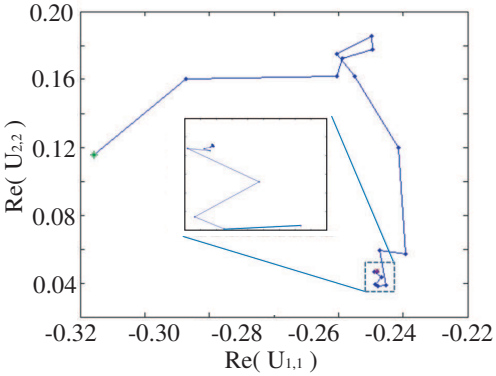

(c)Hybrid method

FIG. 1: (Color Online) Characteristic search trajectories for the three algorithm for the same initial density matrix ρ and initial unitary matrix U for the case of a two-qubit system. The trajectory is projected into the two-dimensional space spanned by the real part of the first two diagonal elements of matrix U.

direction $d^{(n)}$ is computed as follows,

$$\begin{aligned} \beta^{(n)} &= \frac{g^{(n)} \cdot g^{(n)}}{g^{(n-1)} \cdot g^{(n-1)}} \\ d^{(n)} &= -g^{(n)} + \beta^{(n)} d^{(n-1)} \text{ for } n > 1 \\ d^{(1)} &= -g^{(1)} \end{aligned} \tag{16}$$

Since both d and g are matrices with complex elements, the inner product in Eq. (16) is defined as $a \cdot a = \sum_i \sum_j a_{ij} a_{ij}{}^*$. The above algorithm ensures that the search direction $d^{(n)}$ is conjugate to not only $d^{(n-1)}$, but to all the previous search directions, if the landscape of the objective function is quadratic. The CG algorithm requires us to find the minimum of the

function along each search direction before beginning the next search direction. This is a one-dimensional minimization problem for function $f(\lambda) = E(\rho, U^{\rm new})$, where $\tilde{U}^{\rm new} = \tilde{U}\, e^{i\,\lambda g^{(n)}}$. We minimize $f(\lambda)$ by evaluating it at three points, $\lambda = 0$ (at no additional cost), $\lambda = 0.1$ and $\lambda = 0.2$, and fit the function to a parabola. In the rare case of $E(\rho, U^{(n)}) > E(\rho, U^{(n-1)})$ (usually less than 5% of the time), the one-dimensional minimization obviously fails. In this case, we simply replace this CG step by a steepest descent step and restart the CG relaxation (resetting $n = 1$).

Fig 1(b) illustrates the trajectory of a typical CG minimization for the same density matrix ρ and initial unitary matrix $\tilde{U}$ as that in Fig. 1(a). As expected, the CG trajectory does not show the zig-zag behavior as in the SD trajectory. As a result, the CG algorithm usually takes less iterations than SD to converge. Unfortunately, the CG trajectory develops chaotic spirals as the minimum is approached, slowing down the convergence. Since each CG iteration requires more than one evaluation of the entanglement function, the overall convergence speed for the CG algorithm is similar compared to that of SD (see Section II F).

E. Hybrid Method

Given the limitations of both SD and CG algorithms, we find that a much more efficient algorithm can be constructed for entanglement minimization when we combine the two together. In particular, it has been suggested that for highly non-quadratic landscape, a good strategy is to reset the CG search direction to the steepest descent direction from time to time. [13] Therefore, in the hybrid method, we separately perform both a steepest descent step and a conjugate gradient step at each iteration. The actual step we take is the one that gives us the lower entanglement value, i.e. by comparing $E(\rho, U_{SD}^{new})$ and $E(\rho, U_{CG}^{new})$. Even though one iteration in the hybrid method is more expensive than both SD and CG, the algorithm is much more efficient because it takes much fewer iterations to converge. As shown in Fig. 1(c), the trajectory from hybrid method does not display either zig-zag or spiral characteristics. We suggest in passing that it would be worthwhile to test the hybrid method to other optimization problems, such as protein folding or *ab initio* calculations, whose objective function has a complex landscape.

F. Comparison of convergence speed

The entanglement of formation between two qubits ($N = 4$) has been derived analytically [6], which can be used as a benchmark for the numerical algorithms. We found that all three gradient search algorithms reach the (global) minimum given by the analytic solution with $M = N = 4$ starting from an aribitrary initial unitary matrix. This indicates that there is only a single minimum for the entanglement as a function of U. While all three methods converge to the correct results in this case, their computation time is different.

The algorithms are tested on $1,000$ randomly generated density matrices and initial unitary matrices (the random measure μ is defined in Section III A). The search iterations continues until the absolute error of the entanglement measured from the analytic result is less than 10^{-12}. The tests are performed using a Matlab program running on a Pentinum II PC. The benchmark results are shown in Table I, which clearly demonstrates the superiority of the hybrid method over the other two. The average computation time for the hybrid method (HM) is 4 to 5 times shorter than that for SD and CG, while the number of iterations is 6 to 8 times smaller. It is also worth noting that SD sometimes requires an exceptionally large number of steps to converge. We therefore limit the total number of iterations for all three algorithms to $10,000$, at which point the algorithm will abort and declare failure if convergence is still not reached. 97 of the $1,000$ test cases failed when SD is used, while none of the cases failed if either CG or HM is used. Thus the average time statistics for SD would become even less favorable compared with the other two had we used an even larger number for the maximum allowed steps. In the following, we will only use HM to collect the statistics of entanglement. The HM program is re-implemented into C++, which is faster than the Matlab version by 2 orders of magnitude.

G. Local and global minima

Because the definition of the entanglement of formation requires the solution of a global minimization problem, it is of interest to find out whether the landscape of the entanglement function have multiple local minima. In the case of two qubits ($N = 4$), we find that the minimization algorithm (hybrid method) always converge to the analytic solution given arbitrary initial unitary matrix U. This indicates that for $N = 4$ there is only a single

TABLE I: Time statistics for the computation of entanglement for $1,000$ randomly generated 4×4 density matrices using the three algorithms: steepest descent (SD), conjugate gradient (CG) and hybrid method (HM). $t_{\rm ave}$ and $t_{\rm std}$ are the average and standard deviation of wall-clock time (in seconds). $\text{step}_{\rm ave}$ and $\text{step}_{\rm std}$ are average and standard deviation of the number of iterations (for SD), or search directions (for CG and HM). The minimization declares failure if convergence is not reached when the maximum iteration limit (10,000 here) is reached. $N_{\rm fail}$ is the number of failure in the $1,000$ test cases.

Method	t_{ave}	t_{std}	step_{ave}	step_{std}	N_{fail}
SD	1.30	3.13	555.26	1337.2	97
CG	1.57	1.84	419.78	484.13	0
HM	0.307	1.15	68.29	250.86	0

minimum which is the global minimum. However, for $N > 4$, we find multiple minima whose number increases with increasing N. Fig. 2 shows the histograms of the local minima found for two density matrices starting from $1,000$ randomly chosen initial unitary matrices (dimension $M \times M$) where we have set $M = N$. The exact values of the these matrices are provided in the supplementary documents on the APS web site. Fig. 2(a) corresponds to the case of two qudits each with 3 independent states, i.e. $N = 3 \times 3 = 9$, for which several discrete local minima are found. The lowest minima is found almost 200 times and it is very likely the global minimum. Fig. 2(b) corresponds to the case of two qudits each with 4 independent states, i.e. $N = 4 \times 4 = 16$, for which more local minima are found. The spread of these local minima is also much larger than the case of $N = 9$.

Theoretically speaking, the dimension of the unitary matrix has to be larger than that of the density matrix with $M = N^2$. In the case of two qubits ($N = 4$), however, we have found that the gradient search algorithm is always able to find the global minimum even with $M = N$. Unfortunately, we found this is no longer the case for $N > 4$. Since the decompositions described by all unitary matrices of a lower dimension is a subset of those described by unitary matrices of a higher dimension, we expect the lowest minimum found among all unitary matrices of dimension $M \times M$ should decrease with increasing M. Therefore, it is of interest to investigate how the lowest minimum value converges with increasing M. Due to the limited computational resource, it is often impossible to try all

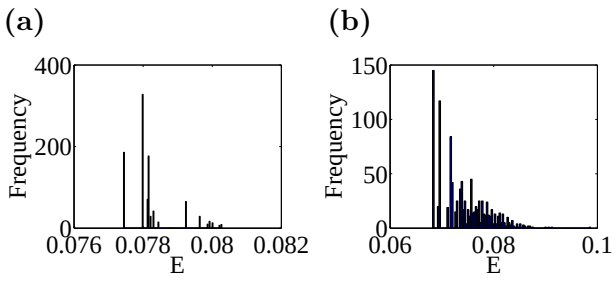

FIG. 2: (Color Online) Histogram of local minima of the entanglement function for two density matrices of dimension $N \times N$, each obtained from gradient searches starting from $1,000$ different initial decomposition matrices of dimension $M \times M$ with $M = N$. (a) $N = 3 \times 3 = 9$. (b) $N = 4 \times 4 = 16$. [17]

possible values of M from N to N^2. For example, for two qudits each having 4 independent states, $N = 4 \times 4 = 16$ and $N^2 = 256$. If we let $M = N^2$ then matrix $\tilde{U}$ would have $65,536$ elements and matrix U would have 4096 elements. This is beyond the range of our current computational power, especially because we still need to try many (e.g. 100) different initial unitary matrices for each chosen M to ensure a fair chance of finding the global minimum.

We have tested the convergence of the lowest minimum as M increases from N to $2N$. When one of the two particles is a qubit (having only two independent states), changing M from N to $2N$ does not change the lowest minimum value by more than 1%. In all other cases, the lowest minimum seems to decay exponentially with increasing M and seem to have converged well before M reaches $2N$. This is a good sign because it suggests that numerically it may not be necessary to ever go to the limit of $M = N^2$. Fig. 3 illustrates this convergence behavior for the case of $N = 4 \times 4 = 16$. The lowest minimum value obtained for different values of M is normalized by the value for $M = N$. The normalized curve is then averaged over several hundred (200 for $N > 10$, 500 otherwise) random density matrices, which leads to the curve in Fig. 3. The normalized and averaged entanglement value is seen to converge exponentially,

$$E(M) = E_0 + \Delta E \, \exp[-\lambda(M - N)] \tag{17}$$

where the rate of convergence λ can be obtained empirically by numerical fitting. To see whether the rate of convergence is large enough to justify stopping M at $2N$, we can use $\delta E = \Delta E \, \exp(-\lambda N)$ as an error estimator. The fitted values for λ and the error estimates

δE for various choices of $N = n_A \times n_B$ are shown in Table II, where n_A and n_B are the number of independent states for particles A and B, respectively. In all the cases we have tested, this error estimator never exceeds 10^{-3}. Notice that the smallness of δE only indicates the self-consistency for stopping M at $2N$. It does not preclude the possibility that a substantially lower minimum can be found for some $M > 2N$. As a compromise between numerical accuracy and computational cost, we use $M = 2N$ for all the calculations in Section III.

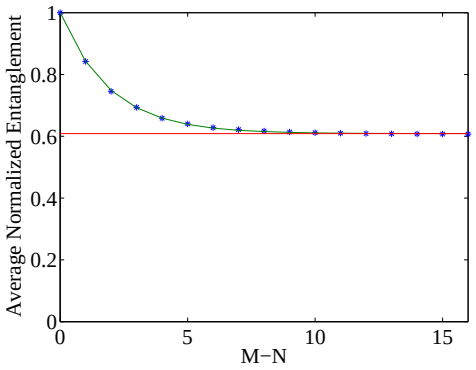

FIG. 3: (Color Online) Minimum entanglement value obtained for different M normalized by the value at $M = N$ and then averaged over several hundred random density matrices for $N = 4 \times 4 = 16$. The data is fitted to an exponential function $E(M) = E_0 + \Delta E \exp[-\lambda(M - N)]$ and the solid line represents E_0.

TABLE II: Fitted value of λ and ΔE in Eq. (17) and error estimate $\delta E = \Delta E \exp(-\lambda N)$ for various choices of $N = n_A \times n_B$ (see text).

N	n_A	n_B	λ	ΔE	$\delta E/E_0$
6	2	3	3.25	0.0005	1.2e-12
8	2	4	1.46	0.0025	2.2e-8
9	3	3	1.68	0.0273	7.0e-9
10	2	5	1.25	0.0046	1.6e-8
12	3	4	1.61	0.187	1.0e-8
15	3	5	0.71	0.257	1.8e-6
16	4	4	0.51	0.393	1.7e-4

III. ENTANGLEMENT STATISTICS IN RANDOM DENSITY MATRIX ENSEMBLE

In this section, we apply the gradient search algorithm developed in the previous section to an ensemble of random density matrices and explore the correlation between entanglement and other easier-to-compute quantities such as participation ratio and negativity.

A. Random density matrix ensemble

Before we can discuss the statistical distribution of the entanglement of randomly distributed density matrices, we first need to define a *measure* in the space of density matrices, i.e. to specify the precise meaning of "randomly distributed". Because there is no standard definition for the measure in the space of density matrices, we follow the definition proposed by Życzkowski [7]. Recall that a density matrix is a positive semi-definite Hermitian matrix with trace equal to one. A density matrix can always be diagonalized by a unitary transformation, $\rho = VDV^\dagger$. Hence a measure μ of density matrix ρ can be constructed from the measure Δ_1 of the diagonal matrix D and the measure ν_H of the unitary matrix V, i.e.,

$$\mu = \Delta_1 \times \nu_H \ . \tag{18}$$

The measure Δ_1 is a uniform distribution on the $(N-1)$-dimensional simplex determined by the trace condition $\sum_i^N D_{ii} = 1$. ν_H is the Haar measure for random unitary matrices. [9] To generate a random density matrix, we first generate a random unitary matrix V according to the Haar measure using the algorithm given in [9]. Another auxiliary random unitary matrix U is generated by the same algorithm and the squared moduli of its first column is used to generate the diagonal elements of matrix D,

$$D_{ii} = |U_{i1}|^2 \tag{19}$$

The random density matrix is obtained by $\rho = VDV^\dagger$.

Using this procedure, we generate $10,000$ density matrices of dimension $N \times N$ for every $N = 4, 6, 8, 9, 10, 12, 15, 16$, as listed in Table III. Analytic solutions are used in the case of $N = 2 \times 2$. In higher dimensions, entanglement is obtained by the hybrid gradient search algorithm with with $M = 2N$ and the convergence criteria is set such that the average of reduction of entanglement over the last 10 consecutive steps is less than 10^{-11}. For each

density matrix, minimization is performed from 10 randomly chosen initial unitary matrices and the lowest minimum value obtained among these 10 runs is used as the (upper-bound) estimate of the global minimum. The entanglement results thus obtained are correlated with other quantities that are believed to be related to entanglement, such as participation ratio and negativity [7, 10, 15].

B. Participation ratio

The participation ratio R of a density matrix ρ is defined as,

$$R(\rho) = \frac{1}{\mathrm{Tr}(\rho^2)} \ . \tag{20}$$

Because $R = 1$ for certain pure states and $R = N$ for totally mixed states ($\rho = I/N$), R can be interpreted as an effective number of pure states in the mixture. Therefore we would expect a decreasing entanglement E for an increasing R. Fig. 4 demonstrates the anti-correlation between entanglement E and participation ratio R. As the participation ratio R grows, especially when R exceeds a certain threshold value, the fraction of states with zero entanglement (i.e. separable states) increases. In other words, purer quantum states (with smaller R) tend to have a smaller probability to be decomposable into factorizable states.

C. Negativity and PPT states

The elements of a density matrix can be specified by $\rho_{jl,j'l'}$ where indices j and j' corresponds to sub-system A and indices l and l' corresponds to sub-system B. A partial transpose of ρ is defined as

$$\left(\rho^{\mathrm{T}_2}\right)_{jl,j'l'} = \rho_{jl',j'l}. \tag{21}$$

in which only the indices for sub-system B are transposed. All of the eigenvalues of the original density matrix ρ are non-negative. However, this is not the case for ρ^{T_2}. The negativity parameter t is defined as a way to quantify the violation of this condition,

$$t \equiv \sum_i^N |d_i'| - 1, \tag{22}$$

where d_i' is the i-th eigenvalue of matrix ρ^{T_2}. Because the partial transpose does not alter the trace, $\sum_i^N d_i' = 1$ is still satisfied. Therefore, if any eigenvalue d_i' is negative, t will

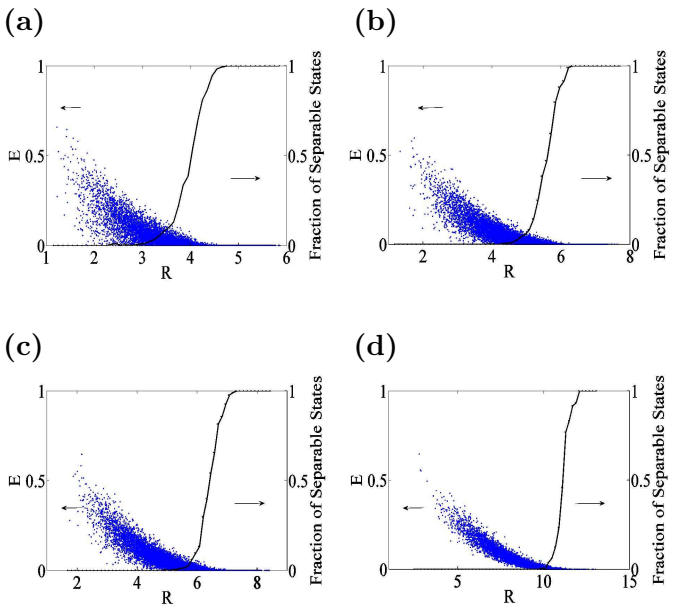

FIG. 4: (Color Online) Dots: correlation between entanglement E and participation ratio R for $10,000$ random $N \times N$ density matrices, where $N = n_A \times n_B$. Solid line: fraction of zero entanglement states for a given participation ratio. (a) $N = 2 \times 2$ (b) $N = 2 \times 3$ (c) $N = 3 \times 3$ (d) $N = 3 \times 5$.

become positive. States with $t = 0$ are called positive partial transpose (PPT) states. It has been shown that a separable state (i.e. $E = 0$) must have $t = 0$. [11] In other words, a separable state must be a PPT state, but the converse is not true. It is also known that all states with participation ratio $R > N - 1$ must have $t = 0$ and $E = 0$. [15] Given these theoretical results, we expect a positive correlation between negativity t and entanglement E, which is indeed supported by our numerical results, as shown in Fig. 5. For all the density matrices that have $R > N-1$, we find that the entanglement reported by the gradient search algorithm is always less than 10^{-9}. This confirms the correctness of the theoretical result as well as the robustness of our numerical algorithm. [15]

Some statistics of our numerical results are summarized in Table III. The correlation function $S(E, t)$ is found to be close to 1 for all the cases, supporting a strong correlation between entanglement and negativity. While it has been shown that for $N = 4$ and $N = 6$, a density matrix is separable ($E = 0$) if and only if it is a PPT state ($t = 0$), for $N > 6$ there exist PPT states with non-zero entanglement. For $N = 8$, Życzkowski [7] estimated the

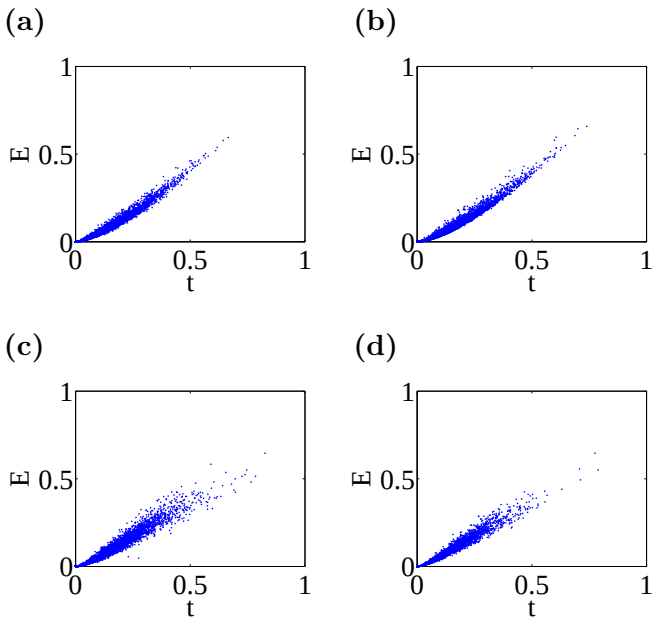

FIG. 5: (Color Online) Correlation between entanglement E and negativity t for $10,000$ random $N \times N$ density matrices, where $N = n_A \times n_B$. (a) $N = 2 \times 2$ (b) $N = 2 \times 3$ (c) $N = 3 \times 3$ (d) $N = 3 \times 5$.

fraction of separable states among PPT states to be only 78.7% [7]. Our numerical results can also be used to estimate the fraction of separable states among PPT states.

Due to limited numerical resolution, we classify all density matrices with $E < 10^{-9}$ as separable states, i.e. $E = 0$. Consistent with the previous report [10], all PPT states are separable for $N \leq 6$. Strikingly, we also found that all PPT states among the $10,000$ randomly generated density matrices (including $N = 8$) have zero entanglement regardless of dimension. This contradicts previous report [7] and suggests that the fraction of separable states among PPT states is close to 100% for the case of $N = 2 \times 4$. The disagreement is mostly due to the faster convergence of our gradient search algorithm, which allows us to use many initial unitary matrices to obtain a better estimate of the global minimum. Nonetheless, our results should not be over-interpreted as: all PPT states are separable states. In fact, Horodecki [14] has provided an example of non-separable PPT states for

TABLE III: Statistics of $1,000$ random density matrices of different dimensions. E_{ave} and t_{ave} is the average entanglement and negativity. $S(E,t) = \mathrm{Cov}(E,t)/[\mathrm{Var}(E)\mathrm{Var}(t)]^{1/2}$ is the correlation between E and t. P_{PPT} is the fraction of PPT states among all the sampled random density matrices.

N	n_A	n_B	E_{ave}	t_{ave}	$S(E,t)$	P_{PPT}
4	2	2	0.0308	0.0568	0.9699	0.630
6	2	3	0.0423	0.0763	0.9732	0.390
8	2	4	0.0482	0.0857	0.9767	0.236
9	3	3	0.0578	0.0969	0.9765	0.165
10	2	5	0.0499	0.0891	0.9799	0.141
12	2	6	0.0531	0.0941	0.9821	0.078
12	3	4	0.0655	0.1070	0.9787	0.071
15	3	5	0.0707	0.1144	0.9798	0.029
16	4	4	0.1573	0.1314	0.9685	0.002

$N = 2 \times 4$,

$$\rho_b = \frac{1}{7b+1} \begin{pmatrix} b & 0 & 0 & 0 & 0 & b & 0 & 0 \\ 0 & b & 0 & 0 & 0 & 0 & b & 0 \\ 0 & 0 & b & 0 & 0 & 0 & 0 & b \\ 0 & 0 & 0 & b & 0 & 0 & 0 & 0 \\ 0 & 0 & 0 & 0 & \alpha & 0 & 0 & \beta \\ b & 0 & 0 & 0 & 0 & b & 0 & 0 \\ 0 & b & 0 & 0 & 0 & 0 & b & 0 \\ 0 & 0 & b & 0 & \beta & 0 & 0 & \alpha \end{pmatrix} \tag{23}$$

where $\alpha = \frac{1}{2}(1+b)$ and $\beta = \frac{1}{2}\sqrt{1-b^2}$. For arbitrary $b \in (0,1)$, this state has negativity $t = 0$, but non-zero entanglement E and participation ratio R. Here we compute the entanglement E as a function of b using the HM algorithm with $M = 2N$. Fig. 6 plots the entanglement E and participation ratio R as functions of b. It is likely that states in this family of density matrices occupies a negligible volume in the ensemble of random density matrices, which is why we did not observe any non-separable PPT states in all of our $10,000$ density matrices (23.6% are PPT states).

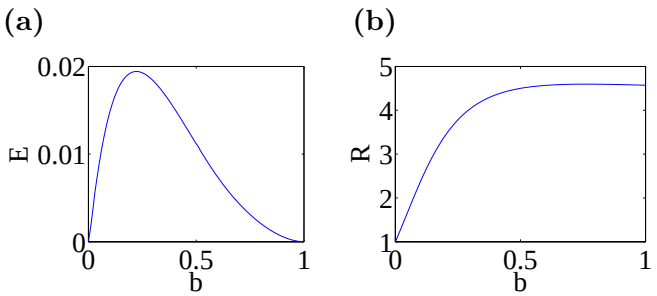

FIG. 6: (Color Online) (a) Entanglement E of the Horodecki state, Eq. (23), as a function of b. (b) Participation ratio R as a function of b.

To test this hypothesis, we generate several ensembles of density matrix by randomly perturbing the Horodecki matrix, Eq. (23), with $b = 0.2$ where the entanglement is close to the local maximum. First, we found that by replacing all zero components in Eq. (23) by a small positive number γ, the resulting density matrix is still a bound entangled state, as long as $0 < \gamma < 0.01\, b$. However, the density matrix is no longer PPT if γ is too large or if the zero components in Eq. (23) are perturbed randomly (i.e. not replaced by the same value γ).

Second, we decompose the Horodecki state into a weighted sum of 16 pure states as in Eq. (7) by using random 16×16 unitary matrices. We then perturb all pure states $\tilde{w}_i$ by adding a random number ξ that is uniformly distributed in the domain $[-\Delta, \Delta]$ to every component. Each perturbed state is then normalized and the normalization constant is multiplied to the assigned probability of this state. The total probability of all states is then renormalized to unity. A new density matrix is obtained by summing up the contributions from each pure state. We have studied four different cases with $\Delta = 0.01b$, $0.1b$, b, $10b$, respectively. $10,000$ random matrices are generated in each case, and the number of PPT states observed are 2, 24, 2816, 4712, respectively. For $\Delta = 0.01b$ and $0.1b$, all the PPT states are bound entangled states. However, for $\Delta = b$ and $10b$, none of the PPT states generated are entangled.

We would like to make the following conjectures based on the above results. First, a small volume of bound entangled states exists at the vicinity of Horodecki matrix, and they are very difficult to find. For example, in the second approach described above, we only found 26 of such states out of $40,000$ random matrices. Second, large perturbations

to the Horodecki matrix lead to an ensemble of density matrices with similar statistical behavior as the ensemble generated earlier in Section.III.A, i.e., all these PPT states have zero entanglement. Given that we are able to generate a few bound entangled states by randomly perturbing the Horodecki matrix (with $\Delta \leq 0.1b$), the fraction of bound entangled states among PPT states can be a finite but very small number.

IV. SUMMARY

We develop a fast gradient search algorithm for the computation of the entanglement of formation for a mixed state, which is defined as the smallest average entanglement among all possible ways to decompose the mixed state into a classical mixture of pure states. This is enabled by the analytic derivatives of entanglement with respect to the unitary decomposition matrix, which are given in Appendix A. A hybrid method, combining steepest descent and conjugate gradient methods, is found to outperform both of them. The fast convergence of the hybrid method allows us to compute entanglement of formation in higher dimensions than what was possible before. Nonetheless, the hybrid method still searches for the local minimum only. In order to estimate the global minimum, we repeat the gradient search several times starting from different random initial conditions and select the lowest local minimum obtained from all the searches. In principle, the gradient search algorithm presented here can be combined with other techniques, such as the simulated annealing [16] or genetic algorithm [8] to expedite the search for the global minimum.

Using the hybrid gradient search algorithm, we obtained entanglement statistics of $10,000$ density matrices with N ranging from 2×3 to 4×4. Anti-correlation is observed between entanglement E and participation ratio R, whereas a strong correlation is observed between E and negativity t. In particular, all the PPT states (density matrices with $t = 0$) in our study are found to be separable ($E = 0$). This suggests a much higher ratio of separable states among PPT states than reported earlier, most likely due to the better convergence of our numerical results.

APPENDIX A: DERIVATIVES OF E WITH RESPECT TO U

Consider the entanglement E as a function of both the density matrix ρ and the decomposition matrix U,

$$E(\rho, U) = \sum_{i=1}^{M} p_i \, E(\rho^{AB(i)}) \tag{A1}$$

where $\rho^{AB(i)} = |\tilde{w}_i\rangle\langle\tilde{w}_i|$ is the density matrix of the pure state $|\tilde{w}_i\rangle$. The entanglement of a pure state is defined through the von Neuman entropy of the partial trace,

$$E(\rho^{AB(i)}) \equiv S(\rho^{A(i)}) = -\mathrm{Tr}\left[\rho^{A(i)} \log_2 \rho^{A(i)}\right] \tag{A2}$$

$$\rho^{A(i)} = \mathrm{Tr}_B\left[\rho^{AB(i)}\right] \tag{A3}$$

In this appendix, we derive the derivative of E with respect to every component of U. It is important to note that the components U_{ij} are complex numbers. We will treat U_{ij} and U^*_{ij} (the complex conjugate) as independent variables. In other words, the change δE with caused by a small change of matrix U can be written as,

$$dE = \sum_{ij} \frac{\partial E}{\partial U_{ij}} \, dU_{ij} + \frac{\partial E}{\partial U^*_{ij}} \, dU^*_{ij} \tag{A4}$$

Computing the derivative of E with respect to U requires the derivatives of both p_i and $S(\rho^{(i)}_A)$ with respect to U, i.e.,

$$\frac{\partial E(\rho)}{\partial U_{kl}} = \sum_{h=1}^{M} \left[\frac{\partial p_h}{\partial U_{kl}} S(\rho^{A(h)}) + p_h \frac{\partial S(\rho^{A(h)})}{\partial U_{kl}} \right] . \tag{A5}$$

The derivative of p_i is easier to obtain,

$$\frac{\partial p_h}{\partial U_{kl}} = \lambda_l U^*_{hl} \delta_{kh} \, , \tag{A6}$$

where λ_l is the eigenvalue of ρ.

To obtain the derivative of $S(\rho^{(i)}_A)$, we need to follow the chain rule,

$$S(\rho^{A(i)}) \to \Lambda_p^{A(i)} \to \rho^{A(i)} \to \rho^{AB(i)} \to |\tilde{w}_i\rangle \to U. \tag{A7}$$

where $\Lambda_p^{A(i)}$ is the p-th eigenvalue of matrix $\rho^{A(i)}$, based on which $S(\rho^{A(i)})$ can be written as,

$$S(\rho^{A(i)}) = -\sum_{p=1}^{n_A} \Lambda_p^{A(i)} \log_2(\Lambda_p^{A(i)}) \tag{A8}$$

Therefore,

$$\frac{\partial S(\rho_A^{(h)})}{\partial \Lambda_p^{A(h)}} = -\log_2(e\Lambda_p^{A(h)}) \tag{A9}$$

Continue with the chain rule,

$$\frac{\partial \Lambda_p^{A(h)}}{\partial U_{kl}} = \sum_{r,s=1}^{N}\sum_{t,u=1}^{n_A} \frac{\partial \Lambda_p^{A(h)}}{\partial \rho_{tu}^{A(h)}} \frac{\partial \rho_{tu}^{A(h)}}{\partial \rho_{rs}^{AB(h)}} \frac{\partial \rho_{rs}^{AB(h)}}{\partial U_{kl}}. \tag{A10}$$

Let $A^{(h)}$ be the matrix that diagonalize the density matrix $\rho^{A(i)}$,

$$\rho^{A(i)} = A^{(h)} D^{A(h)} A^{(h)\dagger} \tag{A11}$$

where $D_{pp}^{A(h)} = \Lambda_p^{A(h)}$. We can show that

$$\frac{\partial \Lambda_p^{A(h)}}{\partial \rho_{tu}^{A(h)}} = A_{tp}^{(h)^*} A_{up}^{(h)} \tag{A12}$$

The middle term in the r.h.s. of Eq. (A10) is either zero or one, depending on the indices t, u, r and s,

$$\frac{\partial \rho_{tu}^{A(h)}}{\partial \rho_{rs}^{AB(h)}} = \sum_{n=0}^{n_B-1} \delta_{(t+n\cdot n_A),r}\delta_{(u+n\cdot n_A),s}, \tag{A13}$$

To find the last term in the r.h.s. of Eq. (A10), we first find that,

$$\frac{\partial (p_h \rho_{rs}^{AB(h)})}{\partial U_{kl}} = \delta_{kh}\, W_{rh}\, V_{sl}^* \tag{A14}$$

Finally,

$$\begin{aligned} p_h \frac{\partial \rho_{rs}^{AB(h)}}{\partial U_{kl}} &= \frac{\partial (p_h \rho_{rs}^{AB(h)})}{\partial U_{kl}} - \rho_{rs}^{AB(h)} \frac{\partial p_h}{\partial U_{kl}} && \text{(A15)} \\ &= \delta_{kh}\left(W_{rh}V_{sl}^* - \rho_{rs}^{AB(h)} \lambda_l U_{hl}^*\right) && \text{(A16)} \end{aligned}$$

Combining all results together, we have

$$\begin{aligned} \frac{\partial E(\rho,U)}{\partial U_{kl}} &= \lambda_l\, U_{kl}^*\, S(\rho^{A(k)}) - \sum_{p=1}^{n_A} \log_2(e\Lambda_p^{A(k)}) \\ &\quad \times \sum_{r,s=1}^{N}\sum_{t,u=1}^{n_A} A_{tp}^{(h)^*} A_{up}^{(h)} \left(W_{rk}V_{sl}^* - \rho_{rs}^{AB(k)}\lambda_l U_{kl}^*\right) \left(\sum_{n=0}^{n_B-1} \delta_{t+nn_A,r}\, \delta_{u+nn_A,s}\right) \end{aligned} \tag{A17}$$

APPENDIX B: STEEPEST DESCENT DIRECTION FOR HERMITIAN MATRIX H

In this appendix, we show that the steepest descent direction for Hermitian matrix H (defined by $\tilde{U} = e^{iH}$) is

$$g = \frac{1}{2}\left[\left(i\tilde{U}^\dagger \tilde{G}^*\right) + \left(i\tilde{U}^\dagger \tilde{G}^*\right)^\dagger\right] \tag{B1}$$

First, recall that we treat U_{ij} and its complex conjugate U_{ij}^* as independent variables. This means that a differential change of E can be written as

$$dE = \sum_{i=1}^{M}\sum_{j=1}^{N} G_{ij}dU_{ij} + G_{ij}^* dU_{ij}^* \tag{B2}$$

where

$$G_{ij} = \frac{\partial E(\rho, U)}{\partial U_{ij}} \tag{B3}$$

is the derivative we obtained in Appendix A. It can be verified that, if matrix U were not subject to any constraints, the steepest descent direction for U_{ij} should be $-G_{ij}^*$, instead of $-G_{ij}$ itself.

To impose the unitary constraint, we let

$$\tilde{U}^{\text{new}} = \tilde{U}\, e^{i\delta H} \tag{B4}$$

where δH is a small Hermitian matrix. Hence the change of matrix $\tilde{U}$ is,

$$\delta\tilde{U} = \tilde{U}^{\text{new}} - \tilde{U} = i\,\tilde{U}\,\delta H \tag{B5}$$

to the first order of δH. For convenience, we define a square matrix $\tilde{G}$ whose first N columns are identical to G, while other columns are filled with zeros. The ensuing change of E is,

$$\begin{aligned} dE &= \sum_{i=1,k=1}^{M}\sum_{j=1}^{N} i\,G_{ij}\tilde{U}_{ik}\delta H_{kj} - i\,G_{ij}^*\tilde{U}_{ik}^*\delta H_{kj}^* \\ &= \sum_{i=1,j=1,k=1}^{M} i\,\tilde{G}_{ij}\tilde{U}_{ik}\delta H_{kj} - i\,\tilde{G}_{ij}^*\tilde{U}_{ik}^*\delta H_{kj}^* \\ &= \sum_{k=1}^{M}\sum_{j=1}^{M}(i\,\tilde{U}^T\,\tilde{G})_{kj}\,\delta H_{kj} + (i\,\tilde{U}^T\,\tilde{G})_{kj}^*\,\delta H_{kj}^* \end{aligned}$$

Since δH is a Hermitian matrix, $\delta H_{kj} = \delta H^*_{jk}$. Hence,

$$\begin{aligned} dE &= \sum_{k=1}^{M}\sum_{j=1}^{M} (i\,\tilde{U}^T\,\tilde{G})_{kj}\,\delta H_{kj} + (i\,\tilde{U}^T\,\tilde{G})^*_{kj}\,\delta H_{jk} \\ &= \sum_{k=1}^{M}\sum_{j=1}^{M} \left[(i\,\tilde{U}^T\,\tilde{G})_{kj} + (i\,\tilde{U}^T\,\tilde{G})^*_{jk}\right]\,\delta H_{kj} \\ &= \sum_{k=1}^{M}\sum_{j=1}^{M} \left[(i\,\tilde{U}^T\,\tilde{G}) + (i\,\tilde{U}^T\,\tilde{G})^\dagger\right]_{kj}\,\delta H_{kj} \\ &= \sum_{k=1}^{M}\sum_{j=1}^{M} \frac{1}{2}\left[(i\,\tilde{U}^T\,\tilde{G}) + (i\,\tilde{U}^T\,\tilde{G})^\dagger\right]_{kj}\,\delta H_{kj} \\ &\quad + \frac{1}{2}\left[(i\,\tilde{U}^T\,\tilde{G}) + (i\,\tilde{U}^T\,\tilde{G})^\dagger\right]^*_{kj}\,\delta H^*_{kj} \end{aligned} \tag{B6}$$

Hence the steepest descent direction for H is,

$$\begin{aligned} g &= -\frac{1}{2}\left[(i\,\tilde{U}^T\,\tilde{G}) + (i\,\tilde{U}^T\,\tilde{G})^\dagger\right]^* \\ &= \frac{1}{2}\left[(i\,\tilde{U}^\dagger\,\tilde{G}^*) + (i\,\tilde{U}^\dagger\,\tilde{G}^*)^\dagger\right] \end{aligned} \tag{B7}$$

ACKNOWLEDGMENTS

We wish to thank Prof. Sandu Popescu and Dr. Patrice E. A. Turchi for first introducing us to the problem of entanglement computation. This work was performed under the auspices of the US Department of Energy by the University of California, Lawrence Livermore National Laboratory under Contract No. W-7405-Eng-48. Seunghwa Ryu acknowledges support from a Weiland Family Stanford Graduate Fellowship.

---

[1] M. A. Nielson and I. I. Chuang, Quantum Computation and Quantum Information, Cambridge University Press (2000).

[2] P. W. Shor, Algorithms for Quantum Computation: Discrete Logarithm and Factoring (1994).

[3] E. Schrödinger, Proc. Cambridge. Philos. Soc. **31**, 555 (1935).

[4] J. S. Bell, Physics **1**, 195 (1964).

[5] C. H. Bennett, D. P. DiVincenzo, J. A. Smolin, and W. K. Wootters, Phys. Rev. A **54**, 3824 (1996).

[6] W. K. Wootters, Phys. Rev. Lett. **80**, 2245 (1998).

[7] K. Życzkowski, Phys. Rev. A **60**, 3496 (1999).

[8] R. V. Ramos, J. Comput. Phys. **192**, 95 (2003).

[9] M. Pozniak, K. Życzkowski, and M. Kuś, J. Phys. **A31**, 1059 (1998).

[10] K. Życzkowski, P. Horodecki, A. Sanpera, and M. Lewenstein, Phys. Rev. A **58**, 883 (1998).

[11] A. Peres, Phys. Rev. Lett. **77**, 1413 (1996).

[12] Payne et al., Rev. Mod. Phys. **64**, 1045 (1992).

[13] E. K. P. Chong and S. H. Żak, An Introduction to Optimization, John Wiley & Sons, INC. (1996).

[14] P. Horodecki, Phys. Lett. A **232**, 333 (1997)

[15] L. Gurvits and H. Barnum, Phys. Rev. A **66**, 062311 (2002).

[16] S. Kirkpatrick, C. D. Gelatt, and Jr., M.P. Vecchi, Science **220**, 4598, 671 (1983).

[17] See EPAPS Document No. [ ] for density matrices examined to obtain the histograms.

[18] $e^{i(H+\delta H)} = e^{iH} \cdot e^{i\delta H}$ only in the limit of infinitesimal δH. But Eq. (13) remains a unitary matrix for arbitrary Hermitian matrix δH.